Cement and Concrete Research 41 (2011) 279–291

Contents lists available at ScienceDirect

Cement and Concrete Research

journal homepage: http://ees.elsevier.com/CEMCON/default.asp

Hydration mechanisms of ternary Portland cements containing limestone powder and fly ash

K. De Weerdt [a,*], M. Ben Haha [b], G. Le Saout [b], K.O. Kjellsen [c,d], H. Justnes [a], B. Lothenbach [b]

[a] SINTEF Building and Infrastructure, 7465 Trondheim, Norway
[b] EMPA, Swiss Federal Laboratories for Material Science and Technology, Laboratory for Concrete and Construction chemistry, 8600 Dübendorf, Switzerland
[c] NTNU, Department of Structural Engineering, 7491 Trondheim, Norway
[d] Norcem AS HeidelbergCement, Setreveien 2, 3991 Brevik, Norway

ARTICLE INFO

Article history:
Received 30 August 2010
Accepted 19 November 2010

Keywords:
Pore solution (B)
SEM (B)
X-ray diffraction (B)
Thermodynamic calculations (B)
Compressive strength (C)

ABSTRACT

The effect of minor additions of limestone powder on the properties of fly ash blended cements was investigated in this study using isothermal calorimetry, thermogravimetry (TGA), X-ray diffraction (XRD), scanning electron microscopy (SEM) techniques, and pore solution analysis. The presence of limestone powder led to the formation of hemi- and monocarbonate and to a stabilisation of ettringite compared to the limestone-free cements, where a part of the ettringite converted to monosulphate. Thus, the presence of 5% of limestone led to an increase of the volume of the hydrates, as visible in the increase in chemical shrinkage, and an increase in compressive strength. This effect was amplified for the fly ash/limestone blended cements due to the additional alumina provided by the fly ash reaction.

1. Introduction

Adding 5% limestone powder to Portland cement has been a point of discussions in the past. Proponents put forward energy savings during production, without impairing the quality of the cement and concrete properties. Whereas the opponents claim that limestone powder is merely an adulterant, leading to a reduction in quality [1,2]. One of the first incentives to allow carbonate additions to Portland cement was given by the oil shortage in the 1970's–1980's. This led to an adaption of the Canadian standard CAN3-A5-M83 permitting 5% limestone powder in Portland cement since 1983, followed by the Brazilian norm NBR-5732 adapted in 1988. The rising focus on greenhouse-gasses in the 1990's added to the motivation and in 2000 the proposal for the European standard EN 197-1 (CEN 2000) was accepted, followed by the ASTM C150 in 2004 and the AASHTO M85 in 2007.

A thorough review on the use of limestone powder in Portland cement is given by Hawkins et al. [3]. The effect of 5% limestone powder addition on short and long term macroscopical properties is generally small. Regarding the compressive strength, both enhanced strength and reduced strength have been reported upon limestone addition. A benefit of the addition of small amounts of carbonate is a reduction of the expansion observed upon sulphate attack, which is most prominent for cements with high C_3A-content [3,4]. It also leads to a reduction of the optimal gypsum content, which may result in a reduction of raw material costs. Some of the beneficial effects of limestone powder are attributed to its filler effect. Some researchers report an acceleration of the C_3S and an incorporation of the calcium carbonate into the C–S–H [5,6]. Additionally, limestone is known to interact with AFm and AFt phases. In an ordinary Portland cement without limestone powder, the C_3A and at a slower rate also the C_4AF will react with the calcium sulphate to form ettringite ($C_3(A,F)\cdot 3CaSO_4\cdot 32H_2O$). Upon depletion of the sulphates, the remaining C_3A and C_4AF will react with the ettringite to form monosulphate ($C_3(A,F)\cdot CaSO_4\cdot 12H_2O$) or hydroxy-AFm solid solution. In the presence of limestone, the AFm-carbonate equivalents such as monocarbonate ($C_3(A,F)\cdot CaCO_3\cdot 11H_2O$) are formed rather than the sulphate containing AFm phases. The AFt-carbonate equivalent has been observed by some researchers [7], but it is unlikely to form in a significant amount at ambient temperatures in a hydrating cements as it is less stable than the AFm phases [8,9]. The decomposition of ettringite to monosulphate when reacting with the remaining C_3A and C_4AF upon sulphate depletion is prevented as monosulphate is less stable than monocarbonate in the presence of limestone. The stabilisation of the voluminous, water rich ettringite instead of the less voluminous monosulphate, gives rise to an increase of the total volume of hydration products [10–13]. If some of the beneficial macroscopic effects observed for limestone additions up to 5%, are due to this chemical interaction, it is obvious that the impact will be greater for cements with a high C_3A and C_4AF content as observed by previous investigations [2].

The previous statements and observations brought the idea to investigate the effect of limestone powder additions on blended fly ash cements. Fly ash has generally higher alumina content than OPC. The reaction of fly ash brings additional alumina, which reduce the

* Corresponding author. Tel.: +47 73594866.
E-mail address: klaartje.de.weerdt@sintef.no (K. De Weerdt).

0008-8846/$ – see front matter © 2010 Elsevier Ltd. All rights reserved.
doi:10.1016/j.cemconres.2010.11.014

sulphate to alumina ratio and therefore increases the impact of limestone powder. Previous studies have documented a beneficial effect on the strength development when a small amount of limestone powder is combined with either fly ash [14], natural pozzolans [15] or slag [11,16,17]. Up to 90 days, the ternary Portland cements containing pozzolans or slag, and limestone had a higher strength than their equivalent composite cements without limestone. The underlying reasons for this effect have not been investigated, except by Hoshino et al. [11] who attributed the observed interaction between slag and limestone powder to changes in the AFm and AFt phases, using XRD-Rietveld analysis.

Several series of experiments investigating ternary Portland cements containing fly ash and limestone powder have been performed to study the effect of OPC or fly ash replacement by limestone powder in respectively OPC and fly ash blended cement [18–23]. Minor replacements of fly ash by limestone powder appeared to have a beneficial effect on the strength development of the tested ternary blended cements. A similar effect was observed for the tested OPC but the effect appeared to be less pronounced [21,22] and in some cases replacing 5% of OPC by limestone powder resulted even in a loss of strength [23].

The aim of this paper is to find out how exactly minor additions of limestone powder affect the hydration of OPC and blended fly ash cement. In order to investigate the effect quantitatively, a multi-method approach was adopted on the four following mixes: 100% OPC, 95% OPC + 5% limestone, 65% OPC + 35% fly ash and 65% OPC + 30% fly ash + 5% limestone.

2. Materials

The materials used in this study are: ordinary Portland clinker, class F siliceous fly ash (FA), limestone powder (L), natural gypsum and crystalline quartz (Q). The chemical composition determined by XRF and the physical properties of the clinker, fly ash, limestone and quartz are given in Table 1. The clinker was interground with 3.7% of natural gypsum and is further referred to as ordinary Portland cement (OPC). The gypsum used has a $CaSO_4 \cdot 2H_2O$ content of 91.4%. The mineral composition of the OPC and the fly ash determined by Rietveld analysis are given in Tables 2 and 3. The $CaCO_3$ content of the limestone, determined by thermogravimetric analysis (TGA), is about 81%. The limestone powder and the fly ash were ground separately in a laboratory ball mill with a capacity of 9 kg. The particle size distribution of OPC, fly ash and limestone powder determined by laser granulometry using a Malvern Mastersizer are given in Fig. 1.

The experimental matrix is given in Table 4. Some additional combinations were tested using quartz powder instead of limestone powder. The crystalline quartz was assumed to be chemically inert and was therefore used to study the filler effect. The quartz powder was obtained by combining 3 different powders, resulting in a particle size distribution similar to the one of limestone powder (Fig. 1).

Table 1
Chemical composition (wt.%) and the physical characteristics of the clinker, fly ash and limestone powder.

	Clinker	Fly ash	Limestone	Quartz
SiO_2	20.0	50.0	12.9	99.4
Al_2O_3	5.4	23.9	2.7	0.3
Fe_2O_3	3.1	6.0	2.0	0.04
CaO	60.6	6.3	42.3	0.02
MgO	2.9	2.1	1.8	–
SO_3	1.5	0.4	–	–
P_2O_5	0.1	1.1	–	–
K_2O	1.2	1.4	0.6	0.04
Na_2O	0.5	0.6	0.5	–
LOI	0.3	3.6	37.7	–
Carbon	–	3.1	–	–
Chloride	0.05	0.0	–	–
Free CaO	1.85	–	–	–
Gypsum	3.7	–	–	–
Blaine surface [m^2/kg]	450*	450	810	–
Density [kg/m^3]	3150*	2490	2740	2650
D_{50} [μm]	11*	14	4	5

* For OPC = clinker + gyspum.

Table 2
Mineral composition of the clinker determined by XRD-Rietveld analysis.

Minerals	[wt.%]
C_2S	19
C_3S	54
C_3A	11
C_4AF	8

Table 3
Mineral composition of the fly ash determined by XRD-Rietveld analysis.

Minerals	[wt.%]
quartz	12.3
calcite	0.4
hematite	0.6
anhydrite	0.4
mullite	18.3
amorphous*	68.0

* Glass and 3% amorphous carbon.

3. Methods

Mortar prisms (40 × 40 × 160 mm) with cement–sand–water proportions of (1/3/0.5) were prepared. The samples were cured in $Ca(OH)_2$ saturated solution at 20 °C. The *compressive and flexural strength* were determined on two mortar prisms for each testing age according to EN 196-1.

About 6 g of paste with water to binder ratio of 0.5 was prepared in a glass vial using a slow stirring IKA-WERKE RW16 mixer. The vial was sealed and loaded into a TAM Air isothermal calorimeter in order to determine the *rate of heat of hydration* during the first 24 h at 20 °C.

Chemical shrinkage at 20 °C was assessed using the method described by Geiker et al. [24].

Cement paste samples were prepared with water to binder ratio of 0.5 and stored at 20 °C in 20 ml sealed plastic vessels for thermogravimetric analysis (TGA), X-ray diffraction (XRD) and scanning electron microscopy (SEM) studies, and 500 ml sealed plastic bottles for pore solution analysis. The samples, used for thermogravimetric

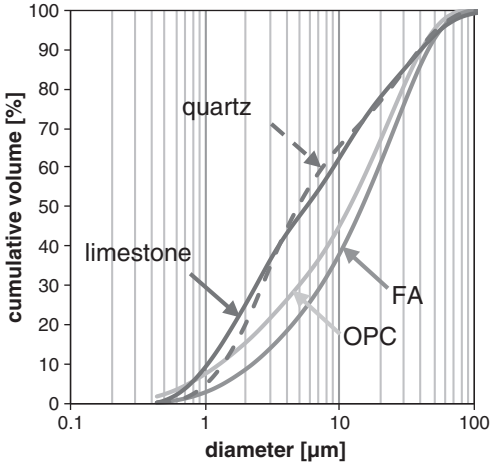

Fig. 1. The particle size distribution of OPC, FA, limestone and quartz determined by laser diffractometry.

Table 4
Experimental matrix in wt.%.

Name	OPC	FA	L
OPC	100	–	–
OPC-L	95	–	5
OPC-FA	65	35	–
OPC-FA-L	65	30	5

analysis and X-ray diffraction, were crushed (<63 μm). The hydration was stopped by solvent exchange using isopropanol during 15 min and flushing with ether.

Thermogravimetric analysis was performed on about 50 mg of the resulting powder by monitoring the weight while heating up from 30 to 980 °C at 20 °C/min and purging with N_2, in a Mettler Toledo TGA/SDTA851. The amount of hydrate water (H) and calcium hydroxide (CH) are expressed as% of the dry sample weight at 550 °C (w_{550}):

$$H = \frac{w_{40} - w_{550}}{w_{550}} \quad (1)$$

and

$$CH = \frac{w_{450} - w_{550}}{w_{550}} \cdot \frac{74}{18} (*) \quad (2)$$

(*) $Ca(OH)_2$ (74g/mol) → $CaO + H_2O$ (18g/mol) weight difference determined using stepwise method.

The exact boundaries for the temperature intervals were read from the derivative curve (DTG). The standard deviation on three independent measurements at all tested ages is not larger than 0.1% for H and 0.2% for CH.

About 3 g of the powder was analysed by *X-ray diffraction* (XRD) using a PANalytical X'Pert Pro MPD diffractometer in a θ–2θ configuration with an incident beam monochromator and CuKα radiation (λ = 1.54 Å). The samples were scanned between 5° and 70° with the X'celerator detector. The *Rietveld analysis* was performed using an external CaF_2 standard according to the method described by Le Saout et al. [25].

Slices of hydrated cement paste samples were cut using a water lubricated saw. They were immediately immersed in isopropanol, kept in it for 30 min and subsequently dried at 40 °C for 24 h. The outer layer of the slice was removed using sand paper. A piece of the slices of the hydrated paste was impregnated using low viscosity epoxy resin, polished down to 0.25 μm, coated with carbon (few nm) and examined using a Philips ESEM FEG XL 30 scanning electron microscopy (SEM). *Backscattered electron images* (BSE) were analysed quantitatively using *image analysis* (IA) to determine the coarse capillary porosity and the degree of reaction of OPC and fly ash [26] by monitoring the changes in their vol.% over time. Sixty images were taken per sample at a magnification of 1600. The minimum pore radius measured corresponds to 0.17 μm. Hence, the coarse porosity measured by this method is only a fraction of the total porosity. *Energy dispersive X-ray spectroscopy* (EDX) was applied to determine the element compositions of the matrix. The Ca/Si ratios, as well as the Al incorporation in the C–S–H, were determined. The analyses were carried out using an accelerating voltage of 15 kV to ensure a good compromise between spatial resolution and adequate excitation of the FeKα peak.

The pore solution was extracted using the steel die method [27]. Immediately after extraction, the solution was filtrated using a 0.45 μm nylon filter. The pH of the pore solution was analysed with a *pH* electrode, calibrated with known KOH concentrations. The concentration of Na, K, S, Ca, Si and Al in the *pore solution* was determined using a Dionex Ion Chromatography system (ICS) 3000 using standards from Fluka.

The hydration of the tested cements was modelled using the Gibbs free energy minimization program, GEMS [28]. The thermodynamic data from the PSI-GEMS database [29,30] was supplemented with cement specific data [31–33]. GEMS computes the equilibrium phase assemblage in a multi-component system based on the bulk composition of the materials. For the sake of simplicity, the part of limestone which is not $CaCO_3$ is considered inert as well as the crystalline part of the fly ash, and the glass phase of the fly ash [26] is assumed to dissolve uniformly.

To check whether the crystalline quartz behaves as an inert material, 50 g of quartz powder was mixed with 50 g of $Ca(OH)_2$ and 100 ml alkaline solution with a pH of 13.5 and KOH:NaOH ratio of 2:1. A small portion of the paste was taken immediately after mixing and the reaction was stopped by solvent exchange using isopropanol and flushing with ether. The rest of the paste was stored under sealed conditions at 20 °C and after 28 days the reaction of the paste was stopped. Both the sample taken immediately after mixing (0 day) and the 28 day old sample were analysed by TGA (see Fig. 2). The quartz seems to be slightly reactive as water was bound in hydration products (increased weight loss up to 350 °C) and calcium hydroxide was consumed (16% decrease in weight loss between 350 and 500 °C). This indicates that the "inert" quartz filler was not completely inert.

4. Results and discussions

4.1. General

Limestone replacement seems to influence the compressive strength of the OPC and OPC-FA mortars. Indeed, the *compressive strength* tends to increase slightly when 5% of respectively OPC or fly ash is replaced by 5% limestone powder from 3 days and onwards, but not after 1 day (Table 5 and Fig. 3). The increase in strength in the presence of 5% limestone is more pronounced for the OPC-FA than for the OPC sample. Replacing part of the OPC by fly ash, results in a slower strength development up to 28 days (Fig. 3). The impact of the replacement with limestone on the *flexural strength* (Table 5) was within the variations of the results.

The effect of limestone and fly ash replacement on the amount of hydrate water (H) and the amount of calcium hydroxide (CH) is determined by TGA analyses. The results (Table 5 and Fig. 4) show that replacing 5% of OPC with limestone powder does not influence the *amount of hydrate water* per OPC but tends to decrease the *CH content* per OPC from 7 days. Replacing 5% of fly ash by 5% of limestone

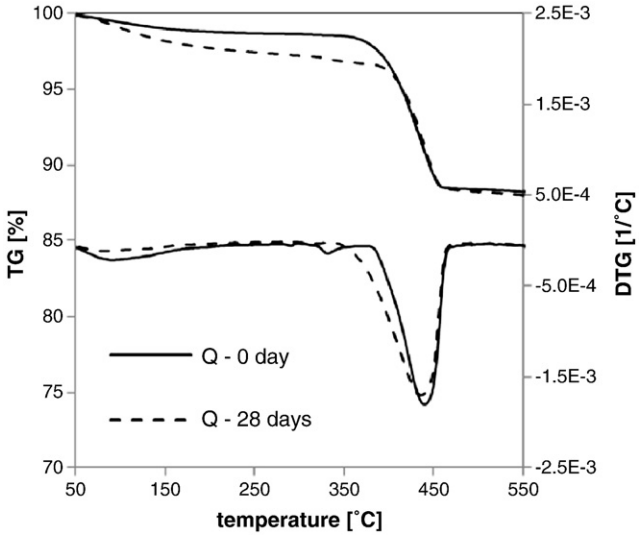

Fig. 2. Weight loss (TG) and derivative weight loss (DTG) curves for 50:50 $Ca(OH)_2$: quartz (Q) mix.

Table 5
The compressive (σ_{comp}) and flexural strength (σ_{flex}), and the amount of hydrate water (H) and calcium hydroxide (CH).

Time [days]	σ_{comp} [MPa]	σ_{flex} [MPa]	H [wt.%]	CH [wt.%]
OPC				
1	22.1	5.3	15.1	12.3
3	31.6	7.2	–	–
7	36.1	7.7	21.9	18.6
28	45.6	7.1	24.1	20.1
90	48.0	6.9	26.3	22.6
180	–	–	28.2	23.4
OPC-L				
1	21.9	5.0	14.6	11.9
3	32.8	7.0	–	–
7	38.1	7.4	21.0	16.3
28	43.9	7.4	23.4	17.9
90	51.5	7.5	25.0	19.3
180	–	–	27.3	20.5
OPC-FA				
1	12.1	3.1	11.2	9.1
3	21.5	4.7	–	–
7	25.7	5.2	16.0	13.1
28	37.8	7.0	18.2	13.5
90	52.3	6.8	19.8	12.5
180	–	–	22.1	12.1
OPC-FA-L				
1	12.4	3.2	11.4	9.6
3	23.8	4.8	–	–
7	28.8	5.7	17.0	12.9
28	39.8	6.0	19.4	12.7
90	55.3	8.5	21.1	11.9
180	–	–	22.9	11.4

powder in OPC-FA however increases the amount of hydrate water per OPC after 7 days and decreases the CH content per OPC after 28 days. The observed decrease in CH when limestone powder is present indicates the formation of hydration products which consume CH e.g. calcium hemicarboaluminate hydrate.

The CH content and the amount of hydrate water per OPC of the fly ash containing cements are initially higher than the OPC and OPC-L cements (Fig. 4), due to the filler effect of the fly ash. Replacing OPC with fly ash increases the effective water to OPC ratio and the fly ash provides additional surface for hydration products to precipitate on, thereby stimulating the OPC reaction. However, the amount of hydrate water relative to the dry binder however decreases, indicating that the filler effect does not compensate for the replacement of the OPC. From 7 to 28 days, the CH content per OPC starts to decrease in the fly ash containing cements as it is consumed by the pozzolanic reaction of the fly ash. The amount of CH was also determined by XRD-Rietveld. The results of both techniques correlated well (±1 wt.% error on both techniques).

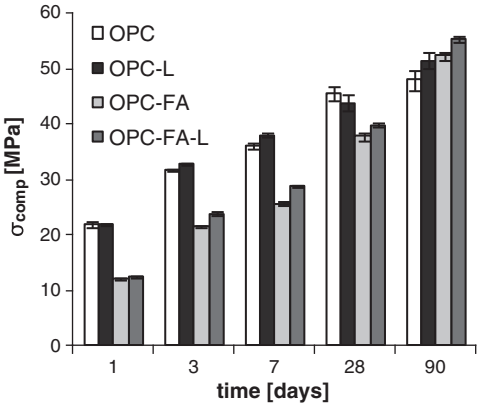

Fig. 3. The compressive strength of mortar samples.

Isothermal calorimetry shows that there is hardly any difference between the heat of hydration per gram OPC evolved during the hydration of OPC or OPC-FA and their limestone containing equivalents during the first 24 h (Fig. 5), which is in agreement with other findings [13]. However, it should be noted that the effect of limestone powder on the heat of hydration emitted depends on the water-to-cement ratio used [34] and the fineness of the limestone powder [35]. The replacement of OPC by fly ash results in an increase and a delay of the maximum *rate of heat of hydration* relative to the OPC content. The shape of the heat evolution curves is also influenced by the presence of the fly ash confirming previous investigations [21]. The cumulative heat per binder emitted during the first 24 h is decreased with the replacement of 35% of OPC with fly ash and/or limestone, (230 → 180 J/g binder). However, the cumulative heat per OPC content increases due to filler effect (230 → 280 J/g OPC) of both limestone and fly ash.

Coupling the previous observations, limestone powder has clearly an effect on the hydration of OPC and OPC-FA reflected by the increase of the compressive strength and amount of bound water and the decrease of calcium hydroxide. However, this effect is not clearly shown from the one day results (e.g. calorimetry and strength), but only prevails later. Microstructural investigations are performed to define qualitatively and quantitatively the effect of limestone powder on the hydrates of both OPC and OPC-FA blended systems.

4.2. Physical or chemical effect?

In order to investigate whether the effect of limestone powder on the hydration of OPC and fly ash blended cements is only physical (additional nucleation sites and higher effective water to cement ratio) or whether there is also chemical effect; limestone powder was replaced with crystalline quartz powder with similar particle size distribution to simulate the physical effect of the limestone.

A new series of experiments including compressive and flexural strength as well as TGA experiments were performed using a different batch of the clinker interground with gypsum. The compressive and flexural strength as well as the amount of hydrate water (H) and calcium hydroxide (CH) after 1 and 28 days of curing at 20 °C, are shown in Table 6 for OPC and fly ash blended cements in which the same amounts of limestone powder and quartz were used. The obtained results are similar to those shown in Table 5.

There is no clear difference between limestone and quartz replacement (5 and 10% of the OPC) in *OPC systems* after 1 day of hydration as shown by both compressive strengths and TGA measurements. Using limestone powder instead of quartz resulted in all cases in a higher compressive strength (about 3–5%) after 28 days of hydration (Table 6). The TGA results after 28 days shows slightly more hydrate water for the limestone powder containing blends (Table 6). The slightly reduced CH content for the quartz containing blends compared to the limestone containing ones is most likely caused by the slight reactivity of the quartz powder (Fig. 2).

For the *fly ash blended cements*, an increase in compressive (8%) and flexural (10%) strength is observed when 5 and 10% of the fly ash is replaced with limestone powder at 28 days (Table 6). Fly ash can be substituted with quartz without impairing the early age compressive and flexural strength. After 28 days more water was bound and slightly less CH was present in the fly ash cements containing limestone powder than in the pure fly ash blended cements, as observed also in Table 5 and Fig. 4. When quartz is used instead of limestone powder in the fly ash blended cements the amount of hydrate water and CH is lower.

The *chemical shrinkage* relative to the OPC content for some of the composite cements containing limestone or quartz is shown in Fig. 6.

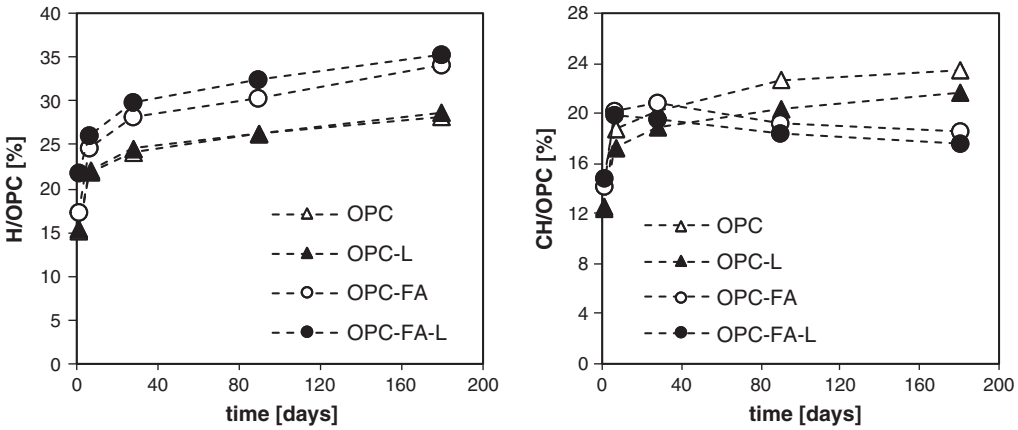

Fig. 4. The amount of hydrate water (H) and calcium hydroxide (CH) relative to the OPC content.

During cement hydration the cement paste exerts chemical shrinkage as the volume of hydration products is smaller than the volume of the reactants. OPC-L and OPC-FA-L have a slightly higher chemical shrinkage per OPC than their limestone free equivalents, OPC and OPC-FA (Fig. 6), indicating that when limestone is present more hydration products are formed, or alternatively different hydrates are formed with even less volume relative to the reactants than the usual hydrates. The fly ash containing cements have a higher total chemical shrinkage per OPC partly caused by the filler effect of the fly ash and partly by the pozzolanic reaction of the fly ash which progresses with time. The quartz (Q) seems to react over time as the slope of the curve after about 12 days is steeper than the ones of 100% OPC and 95% OPC + 5% L. The chemical shrinkage per OPC for the 65% OPC + 30% FA + 5% L and 65% OPC + 30% FA + 5% Q is similar. The fact that the chemical shrinkage of 65% OPC + 35% FA is slightly higher than 65% OPC + 35% Q indicates that the fly ash is more reactive than the quartz.

4.3. Hydration

4.3.1. Anhydrous phases

In order to investigate whether the observed effect of the limestone powder on the mechanical properties of the OPC and the fly ash blended cements is due to a promotion of the clinker hydration, the hydration of clinker phases was monitored by XRD-Rietveld analysis at 0, 1, 7, 28, 90 and 180 days.

The evolution of the anhydrous clinker phases over time is shown in Table 7. *Alite* appears to react fast: more than 70% has reacted after 1 day and more than 90% after 7 days for all tested combinations. The faster reaction of the clinker phases observed in the presence of FA can be attributed to the filler effect of fly ash [36–39]. There is no large difference between OPC-FA and OPC-FA-L concerning the alite hydration, which could explain the observed effect on the compressive strength, bound water and CH of limestone powder on the blended fly ash cement. The content of the aluminate and ferrite phases in the pastes are rather low and their relative error is large, rendering the interpretation of these results difficult. The trends indicate a faster reaction of aluminate and ferrite in the FA containing mixtures. From 28 days, the fly ash tends to retard the reaction of belite in the FA blended pastes confirming the previous reported results [37,39,40]. The overall % of OPC reacted as function of time is similar for all tested combinations.

The degree of hydration of the clinker was also determined by SEM-IA (Fig. 7). Compared to the results from XRD-Rietveld analysis (Table 7), SEM-IA slightly overestimates the degree of reaction of the OPC at early age compared to XRD-Rietveld analysis, possibly due to the omission of small anhydrous grains not detected by SEM-IA. Overall, there is a reasonable agreement between two techniques.

The observed enhancing effect of limestone on the strength, TGA weight loss and chemical shrinkage of the OPC-FA cement might also be caused by a promotion of the fly ash reaction. The degree of

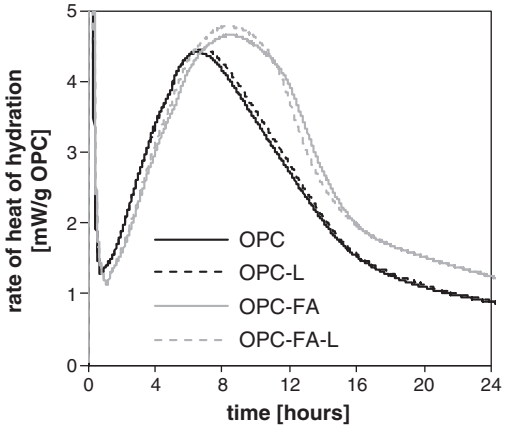

Fig. 5. The rate of heat of hydration relative to the OPC content.

Table 6
Comparing compressive (σ_{comp}) and flexural strength (σ_{flex}), hydrate water (H) and calcium hydroxide (CH) when replacing limestone powder with crystalline quartz.

	Time [days]	σ_{comp} [MPa]	σ_{flex} [MPa]	H [wt.%]	CH [wt.%]
LIMESTONE (L)					
100OPC	1	22.9	4.9	13.6	13.7
	28	47.5	7.9	22.9	21.2
95OPC-5L	1	21.4	4.9	13.2	13.2
	28	46.6	7.7	23.1	20.0
90OPC-10L	1	21.7	4.8	13.3	13.3
	28	45.5	8.0	22.2	19.1
65OPC-35FA	1	12.3	3.0	10.2	10.6
	28	38.3	6.8	17.4	15.0
65OPC-30FA-5L	1	13.2	3.3	10.5	10.6
	28	41.2	7.6	18.5	14.4
65OPC-25FA-10L	1	13.3	3.2	10.3	10.5
	28	41.2	7.9	18.5	14.5
QUARTZ (Q)					
95OPC-5Q	1	20.6	4.8	13.6	13.5
	28	44.4	7.6	22.5	19.4
90OPC-10Q	1	20.8	5.0	13.4	13.2
	28	44.0	7.6	21.6	18.6
65OPC-30FA-5Q	1	12.7	3.4	11.2	11.3
	28	38.5	6.7	18.1	13.9
65OPC-25FA-10Q	1	12.8	3.2	10.4	10.5
	28	38.7	6.8	16.5	12.2

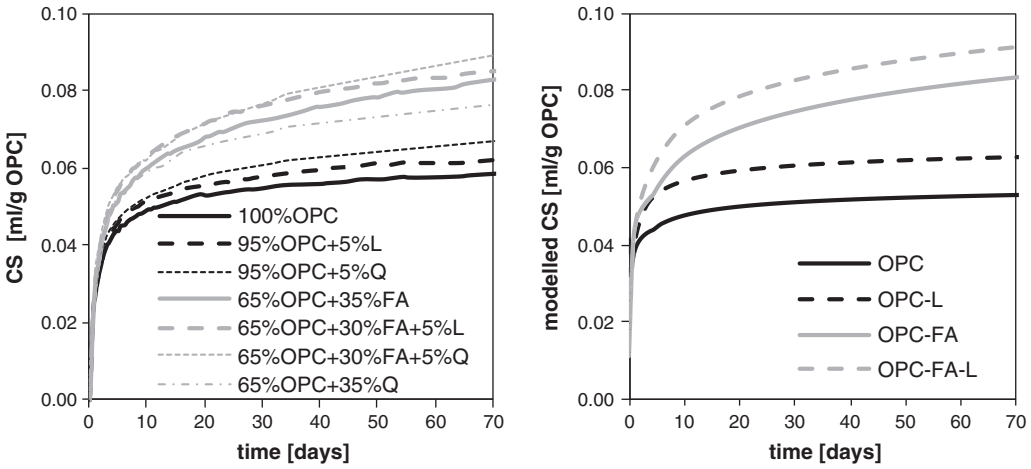

Fig. 6. The measured and modelled chemical shrinkage (CS) relative to the OPC content.

reaction of the fly ash was quantified using SEM-IA as reported in a previous study [26]. Limestone powder does not seem to accelerate the fly ash reaction; the fly ash degree of reaction is similar in both OPC-FA and OPC-FA-L (see Fig. 7).

4.3.2. Hydration products

In order to study the difference in hydration products formed by the tested composite cements, their XRD patterns are compared. The main difference in the XRD-patterns can be seen at low angles, where the main peaks of the AFm and AFt phases are found (Fig. 8). After 1 day of hydration, the patterns are similar for all tested cements: ettringite (9.1° 2θ) and ferrite (12.2° 2θ) are observed. In the absence of limestone powder, the remaining aluminates react with the ettringite to form monosulphate (Ms 9.8° 2θ) [41] after all gypsum is consumed according to:

$$2\ C_3A + C_6A\underline{S}_3H_{32} + 4\ H \rightarrow 3\ C_4A\underline{S}H_{12} \quad (3)$$

Table 7
Content of calcium hydroxide (CH), ettringite, amorphous phases, anhydrous clinker phases relative to the dry content in wt.% determined by XRD-Rietveld analysis.

	Time [days]	CH	Ettringite	Amorphous*	C_3S [wt.%]	C_2S	C_3A	C_4AF	%OPC reacted
OPC	0	–	–	–	55.3	18.9	10.7	8.1	–
	1	12.6	9.8	46.2	15.3	17.8	5.9	5.9	51.7
	7	18.9	10.1	61.3	6.5	17.1	2.5	3.7	68.0
	28	19.0	9.1	71.9	4.5	15.5	1.5	2.5	74.3
	90	21.8	7.4	77.2	2.0	8.2	1.5	2.5	84.7
	180	21.9	8.8	79.6	1.4	6.5	1.5	2.7	87.1
OPC-L	0	–	–	–	52.5	18.0	10.2	7.7	–
	1	11.5	9.0	48.4	13.0	16.7	5.5	5.5	54.0
	7	18.0	9.6	57.1	6.1	15.5	1.8	3.5	69.6
	28	18.3	10.4	62.0	2.9	13.4	1.3	2.5	77.3
	90	18.8	9.9	68.7	2.2	7.8	1.4	2.2	84.5
	180	21.0	11.0	67.9	1.6	5.8	1.4	2.2	87.6
OPC-FA	0	–	–	23.8	33.2	12.2	7.0	5.2	–
	1	8.7	9.0	52.4	9.2	12.2	3.8	4.0	49.1
	7	14.0	7.4	62.6	2.4	11.6	0.8	2.5	69.8
	28	13.7	7.5	69.3	–	10.6	–	1.6	79.0
	90	12.5	6.6	71.2	–	7.8	–	1.5	84.0
	180	11.3	6.6	76.5	–	7.1	–	–	87.6
OPC-FA-L	0	–	–	20.4	33.2	12.2	7.0	5.2	–
	1	8.8	9.3	49.5	8.8	12.0	3.8	3.8	50.8
	7	13.5	9.2	58.4	1.8	11.6	0.7	2.1	71.6
	28	12.8	9.5	67.3	0.6	9.3	–	–	82.8
	90	12.2	10.5	63.0	–	7.3	–	–	87.4
	180	10.8	10.9	69.5	–	6.1	–	–	89.5

* Amorphous = C–S–H + AFm + amorphous content fly ash.

Thus less ettringite is observed in the blends without limestone (Fig. 8). Additionally, another broad peak is observed between Ms and Hc, which might be associated with a carbonate and sulphate containing hydroxy-AFm (AFm*) [13,41].

From 7 days on, AFm* is observed in OPC and OPC-FA. In the OPC-FA blend monosulfate is (Ms) is clearly visible after 28 days.

For the limestone containing combinations, the remaining aluminates will react with calcium carbonate to form a combination of mono- and hemicarbonate (Mc at 11.7° 2θ and Hc at 10.8° 2θ) as observed in Fig. 8 for OPC-L and OPC-FA-L. In this case ettringite does not decompose in reaction with C_3A (Eq. 3):

$$C_3A + C\underline{C} + 11\ H \rightarrow C_4A\underline{C}H_{11} \quad (4)$$

$$C_3A + 0.5\ C\underline{C} + 0.5\ CH + 11.5\ H \rightarrow C_4A\underline{C}_{0.5}H_{12} \quad (5)$$

After 7 days and longer a relatively large peak for hemicarbonate is observed, which decreases with time as monocarbonate forms instead in the OPC-L and OPC-FA-L blends. This might be due to the limited solubility/slow dissolution of the limestone powder.

It should be noted that the calcium hydroxide is consumed during the formation of hemicarbonate (Eq. (5)) which is in line with the observed relative decrease in CH determined by TGA when 5% of the OPC or fly ash is replaced by 5% limestone powder.

SEM-EDX and TGA measurements shown in Fig. 9 confirm the changes in the AFm phases: when limestone is present Mc and Hc are formed instead of Ms, which is in agreement with XRD data discussed previously.

The fly ash blended cements have higher amount of AFm phases relative to the OPC content due to the additional alumina provided by the reaction of the fly ash and to a smaller extent due to the acceleration of the hydration of the aluminate phase of the OPC (Fig. 8).

Rietveld analysis was used to quantify the portlandite, ettringite and the amount of amorphous phases (Table 7). AFm phases are not quantified due to their ill-crystalline structure, their relatively low amount and the lack of data concerning some structures such as hemicarbonate or hydroxyl AFm. Somewhat more ettringite and slightly less portlandite were observed in the samples containing limestone. The presence of FA increased the amount of ettringite per g OPC and decreased the amount of portlandite over time.

The composition of the C–S–H is characterised by SEM-EDX. The Ca/Si ratio and Al/Si ratio of OPC and OPC-L are constant over time with a mean Ca/Si $\approx 1.8 \pm 0.1$ and Al/Si $\approx 0.06 \pm 0.01$. For OPC-FA and OPC-FA-L the ratios change with time: the Ca/Si ratio decreases from ≈ 1.7 at 1 day to ≈ 1.4 at 140 days, and the Al/Si ratio increases

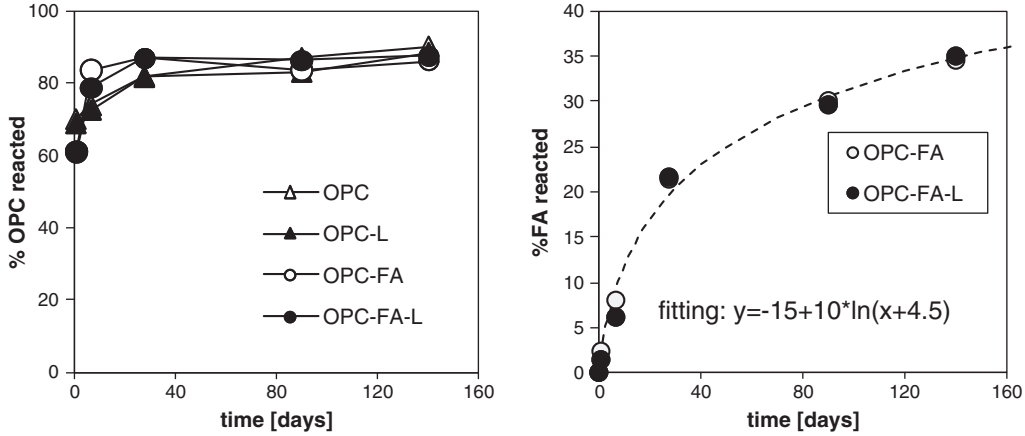

Fig. 7. Percentage of OPC and FA reacted as a function of time both determined by SEM-IA.

respectively from ≈0.06 to ≈0.13 indicating the formation of a more Si rich C–S–H which incorporates more aluminium. The lower Ca/Si and higher Al/Si ratios in the presence of fly ash after longer reaction times agree well with the values found in literature [36,42,43]. The C–S–H present in the OPC-FA blends shows a significant variation in the composition. EDX analysis indicates a large spread of the Ca/Si ratio of the C–S–H from 1.2 to 2.2. This agrees with the findings of other studies, where an inhomogeneous microstructure with large differences in the hydrates and the C–S–H composition are found near fly ash particles, in the outer product or in the inner products near the clinker grains [43–45].

4.3.3. Pore solution

The *pore solution* of the different tested cements was analysed after 1, 28, 90 and 140 days of curing. The different concentrations are given in Table 8. The sulphate concentration and the pH are plotted as a function of time in Fig. 10. For OPC and OPC-L, the Na and K concentration and the pH values increase over time. The pore solution of the fly ash containing cements have lower pH and alkali concentrations than OPC and OPC-L mixes, as reported by previous studies [43,46–48]. Initially, this is due to the dilution of OPC by fly ash. However, after more than 28 days, the alkali concentrations decrease for the fly ash containing combinations indicating an incorporation of alkali in the hydration products formed by the fly ash [43,48,49]. The Ca, Si and Al of both OPC and OPC-L are not significantly different. The Ca-concentration in the pore solution of the OPC-FA and OPC-FA-L mixes, on the other hand, shows a clear decrease, most likely associated with the calcium hydroxide consumption during the pozzolanic reaction of the fly ash observed by TGA and XRD-Rietveld (Fig. 4 and Table 7). The Si and Al concentrations are rather low and are thereby limited in accuracy; however a slight increasing trend with time might be observed for the fly ash containing cements as observed previously [43].

The main difference in pore solution composition between OPC and OPC-FA, and the limestone containing equivalents is the sulphate concentration (Fig. 10). After 7 days the concentration is almost twice as high in the limestone containing mixes than in the ones without limestone, indicating a change in the sulphate containing AFm and AFt phases. The same observations on OPC systems were reported previously [13]. Replacing OPC with fly ash considerably lowers sulphate concentrations, more than what would be expected from the OPC dilution. The chemical reasons for that observed strong decrease of sulphate concentrations are not clear. Possibly, the increase of the total Al_2O_3/SO_3 ratio in the fly ash containing blends is responsible for the observed lower sulphate concentrations in the pore solutions.

Based on the measured concentrations, saturation indices (SI) were calculated. The use of saturation indices can be misleading when comparing phases which dissociate into a different number of ions, thus “effective” saturation indices were calculated by dividing the saturation indices by the number of ions participating in the reactions to form the solids as described by Lothenbach et al. [13]. A positive saturation index implies oversaturation and thereby possible precipitation of the solid; a negative value indicates undersaturation, meaning that the solid cannot form or dissolves. The effective SI for hemi- and monocarbonate has been calculated assuming saturation of the pore solutions with respect to calcite. The effective SI's for

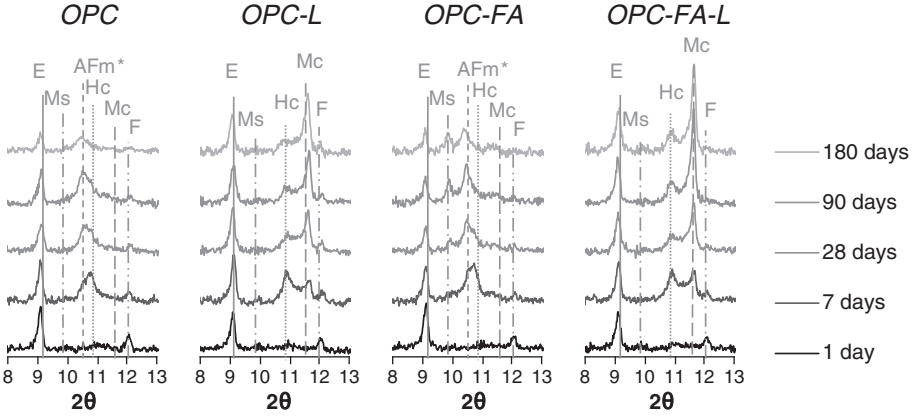

Fig. 8. XRD-patterns for the different tested blends at 1, 7, 28, 90 and 180 days. The main peaks of ettringite (E), monosulphate (Ms), possibly a sulphate and carbonate containing hydroxy-AFm(AFm*), hemicarbonate (Hc), monocarbonate (Mc) and ferrite (F) are indicated.

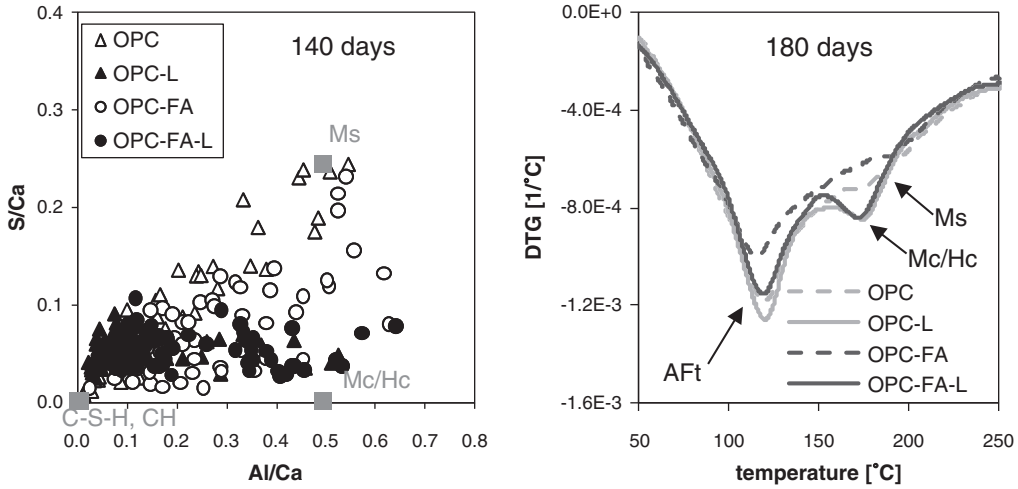

Fig. 9. EDX and TGA analysis of respectively 140 and 180 day old paste samples indicating changes in the composition of the AFm phases.

portlandite, gypsum, ettringite, monosulphate, monocarbonate and hemicarbonate at 1, 7, 28, 90 and 140 days are given in Table 8. Gypsum is under-saturated for all tested combinations. After 28 days and longer portlandite is under-saturated in the fly ash containing blends, due to its consumption by the pozzolanic reaction of the fly ash. This under-saturation is consistent with the slow dissolution of portlandite in the FA containing samples as observed by TGA and XRD (Fig. 4 and Table 7). Ettringite is over-saturated at all times for the OPC, OPC-L and OPC-FA-L samples. Ettringite is under-saturated in the OPC-FA (without limestone) after more than 28 days indicating that ettringite slowly dissolves in this blend. Generally, the effective SI of ettringite is higher in the limestone containing samples. Monosulphate is near saturation for all blends. Mono- and hemicarbonate are near saturation for both limestone containing combinations (except for hemicarbonate for the OPC-FA-L blend at 90 and 140 days).

The pore solution analysis indicates the presence of ettringite and AFm phases as well as the consumption of portlandite in the FA containing blends due to the pozzolanic reaction with the fly ash.

4.3.4. Porosity

The *porosity of the cement paste* has been found to be lower when a small amount of limestone powder is added to OPC [50]. Relative to the aluminate content, ettringite ($C_6A\underline{S}_3H_{32}$) is more voluminous than monosulphate ($C_4A\underline{S}H_{12}$): 707 cm^3/mol versus 309 cm^3/mol at 25 °C [33]. As limestone powder stabilizes the ettringite and prevents the transformation to monosulphate, the total volume of hydration products relative to the OPC content will increase. This volume increase of the hydration products might lead to a reduction in porosity that more than compensates the replacement of OPC by limestone powder.

Table 8
Composition pore solution and effective saturation indices for calcium hydroxide (CH), gypsum, ettringite (Ett), monosulphate (Ms), monocarbonate (Mc) and hemicarbonate (Hc).

Time [days]	Concentration in pore solution [mmol/l]								Effective saturation index					
	Na	K	Ca	S	Si	Al	OH^-	pH	CH	Gypsum	Ett	Ms	Mc	Hc
OPC														
1	131	315	1.1	4.2	0.43	0.22	653	13.7	0.05	−1.35	0.11	0.03	–	–
7	196	417	1.5	6.3	0.37	0.17	699	13.8	0.16	−1.27	0.17	0.09	–	–
28	244	495	1.0	9.3	0.33	0.17	675	13.7	0.14	−1.31	0.13	0.05	–	–
90	274	534	1.4	10.9	0.34	0.23	699	13.8	0.20	−1.23	0.20	0.12	–	–
140	302	565	1.0	13.0	0.30	0.33	627	13.7	0.15	−1.3	0.17	0.10	–	–
OPC-L														
1	258	443	1.5	6.3	0.37	0.21	589	13.7	0.18	−1.31	0.17	0.10	0.19	0.27
7	244	497	1.8	12.8	0.31	0.25	653	13.7	0.22	−1.12	0.28	0.18	0.24	0.36
28	258	515	0.9	17.1	0.29	0.23	631	13.7	0.12	−1.21	0.17	0.07	0.15	0.18
90	274	537	1.2	25.1	0.30	0.21	631	13.7	0.16	−1.09	0.23	0.12	0.17	0.22
140	279	532	1.2	27.6	0.29	0.31	677	13.7	0.17	−1.05	0.28	0.16	0.21	0.30
OPC-FA														
1	223	310	2.0	1.2	0.22	0.16	459	13.6	0.19	−1.51	0.10	0.07	–	–
7	223	303	1.6	1.3	0.16	0.13	493	13.6	0.15	−1.54	0.05	0.02	–	–
28	228	271	1.2	1.6	0.26	0.10	459	13.6	0.09	−1.55	0.00	−0.05	–	–
90	165	241	0.5	2.6	0.48	0.15	368	13.5	−0.08	−1.59	−0.08	−0.14	–	–
140	151	227	0.7	2.6	0.53	0.27	303	13.4	−0.07	−1.53	−0.01	−0.07	–	–
OPC-FA-L														
1	158	313	2.2	1.7	0.21	0.14	442	13.5	0.18	−1.38	0.15	0.09	0.19	0.28
7	184	336	1.9	4.1	0.17	0.13	475	13.6	0.17	−1.25	0.19	0.10	0.18	0.24
28	193	297	1.2	5.9	0.28	0.16	426	13.5	0.08	−1.27	0.14	0.04	0.12	0.12
90	176	251	0.7	7.2	0.45	0.16	368	13.5	−0.04	−1.32	0.06	−0.06	0.04	−0.06
140	151	235	0.6	6.5	0.42	0.22	278	13.3	−0.07	−1.34	0.06	−0.05	0.05	−0.06

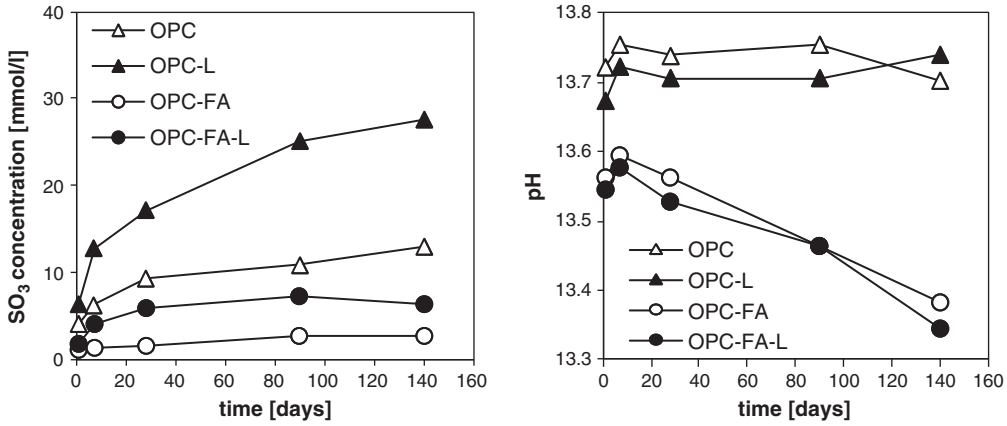

Fig. 10. SO_3 concentration and the pH in the pore solution a function of time.

Image analysis (IA) of backscattered electron (BSE) images taken by a scanning electron microscope (SEM) is used to study the changes of the coarse porosity (Fig. 11). Based on the magnification applied, only coarser pores >0.17 μm are included. In the case of OPC and OPC-L the porosity reduces up to 28 days after which it stays approximately constant, indicating that most of the OPC has reacted within the first 28 days. The initial coarse porosity in the OPC-FA and OPC-FA-L blend is higher and decreases more slowly up to 90 days to values slightly lower than observed for the OPC samples. The coarse porosity does not change significantly between the 90 and 140 days in the FA blended systems.

The relationship between compressive strength and coarse porosity for all tested mixes is presented in Fig. 12 indicating a clear negative correlation between porosity and compressive strength. This suggests that the coarse porosity dominates the compressive strength, independent of the mix designs, which is in agreement with the previous observations [51]. The presence of limestone or FA does not alter the relation between coarse porosity and compressive strength.

4.4. Thermodynamic modelling

4.4.1. Hydrate assemblage

The changes in the hydrate assemblage were calculated based on the observed dissolution of the anhydrous phases. The dissolution of the clinker phases was mathematically described using the Parrot and Killoh equations [52]. The parameters of the equations were adapted to fit the XRD-Rietveld results. The fly ash reaction was expressed using a function fitted to the data obtained in a previous study [26] shown in Fig. 7. Hence, the composition of the hydrate assemblage was predicted based on the degree of reaction of the OPC and the fly ash as a function of the time assuming thermodynamic equilibrium at each stage of the hydration. Some assumptions were introduced while modelling:

- The glassy phase of the fly ash was assumed to dissolve uniformly.
- In the model the formation of monocarbonate was predicted, while by XRD the formation of hemicarbonate instead of monocarbonate was observed at early hydration times (Fig. 8). It is unclear whether the formation of moncarbonate is slower than the formation of hemicarbonate or whether the dissolution of the limestone powder is too slow.
- The EDX results show that the Al-incorporation and the Ca/Si ratio of the C–S–H changes over time for the fly ash containing cements as mentioned before. However, the composition of the C–S–H is kept constant over time. For C–S–H in OPC-FA and OPC-FA-L an Al/Si ratio of 0.13 was used.

The predicted hydrates include C–S–H, CH, AFt and AFm phases including a small amount of hydrotalcite-like phases as shown in Fig. 13. When comparing OPC and OPC-FA with their limestone containing equivalents, the presence of limestone leads to the formation of monocarbonate thus indirectly stabilising ettringite. In the absence of limestone the formation of monosulphate is predicted and a reduction of the amount of ettringite with time (Fig. 13). In the OPC-FA in addition the formation of hydrogarnet is predicted after longer hydration times. Qualitatively these results agree well with experimental results shown in Fig. 8.

In the OPC-FA and OPC-FA-L blends a considerable part of the OPC is replaced by fly ash. OPC reacts faster than the fly ash (Fig. 7), so

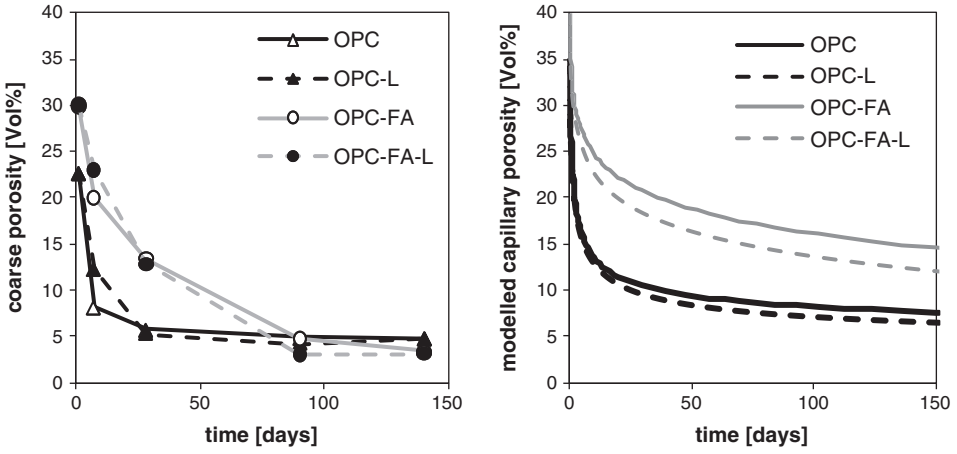

Fig. 11. Coarse porosity determined by SEM-IA (error<2–3%) and modelled capillary porosity.

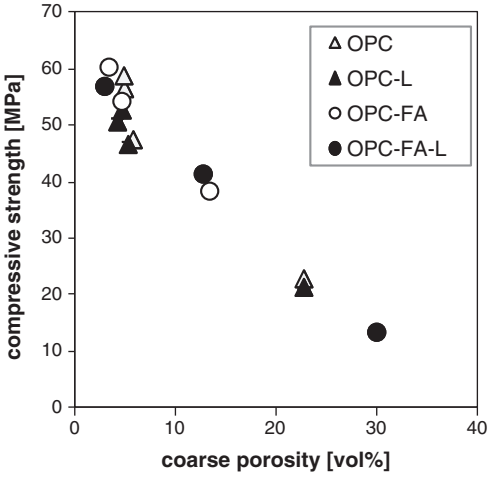

Fig. 12. Relation between compressive strength (error<2%) and coarse porosity determined by SEM-IA (error<2–3%).

initially fly ash acts as an adulterant for OPC. As the fly ash reacts over time, it will introduce additional silicates and alumina to the system. The silicates will react with the portlandite and form additional C–S–H. The alumina will partly be incorporated in the C–S–H and partly in AFm and AFt phases.

The total gypsum content is lower in OPC-FA and OPC-FA-L as gypsum is part of the OPC. The additional alumina provided by the fly ash will therefore lower the SO_3-alumina ratio. Hence, relatively more AFm than AFt phases are formed over time in the fly ash containing blends (see Fig. 13). This amplifies the effect of the limestone powder on the system as limestone interacts with the AFm phases, thereby giving rise to a larger increase in solid volume.

The mass percentage of ettringite, amorphous hydrates and CH determined by Rietveld analysis are compared with the predicted ones (Fig. 14). In the case of OPC and OPC-L, the *CH content* was overestimated by the model, most likely due to differences between the real (Ca/Si = 1.8) and the modelled (Ca/Si = 1.6) C–S–H composition. The model slightly underestimates the CH content for OPC-FA and OPC-FA-L at 28 and 90 days, as:

i) The C–S–H in the OPC-FA(-L) samples shows a lower Ca/Si of 1.4 than the modelled C–S–H (Ca/Si = 1.6). The C–S–H formed in the OPC-FA (−L) blends shows a significant variation in the composition, low Ca/Si C–S–H forms near the FA particles while in other places portlandite is still present. In contrast to these experimental observations, the modelled C–S–H has a constant Ca/Si ratio of 1.6 as the model calculates only bulk properties. The presence of even small quantities of portlandite leads to the stabilisation of high Ca/Si C–S–H.
ii) The dissolution of portlandite may proceed more slowly than the reaction of the FA. The pore solution after 90 and 140 days is undersaturated with respect to portlandite (Table 8), indicating only a slow portlandite dissolution. Due to the inhomogeneous distribution of the C–S–H and the portlandite in the cement matrix, portlandite does persist in some parts of the microstructure while in other areas a low Ca/Si C–S–H is formed.

The *amorphous content* is slightly overestimated for all tested combinations, mainly due to the difference between the modelled and

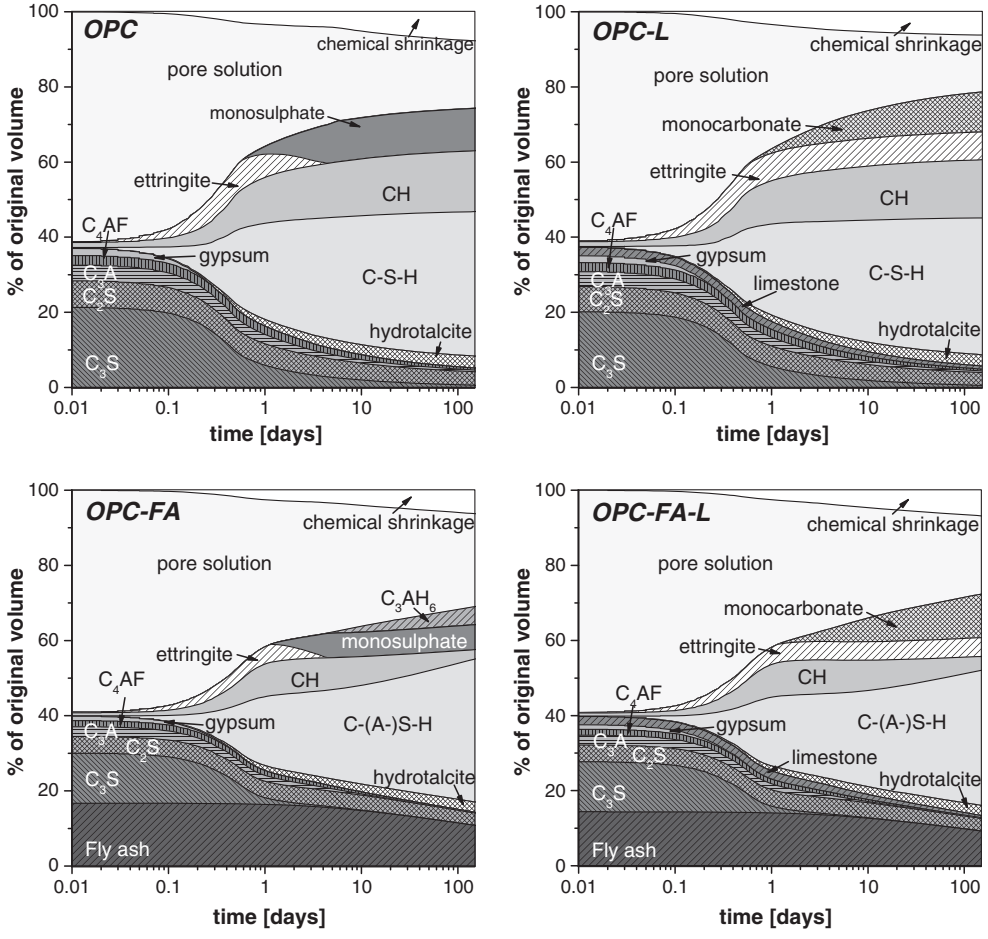

Fig. 13. The volume of the different phases as function of time in hydrating cement pastes modelled by GEMS.

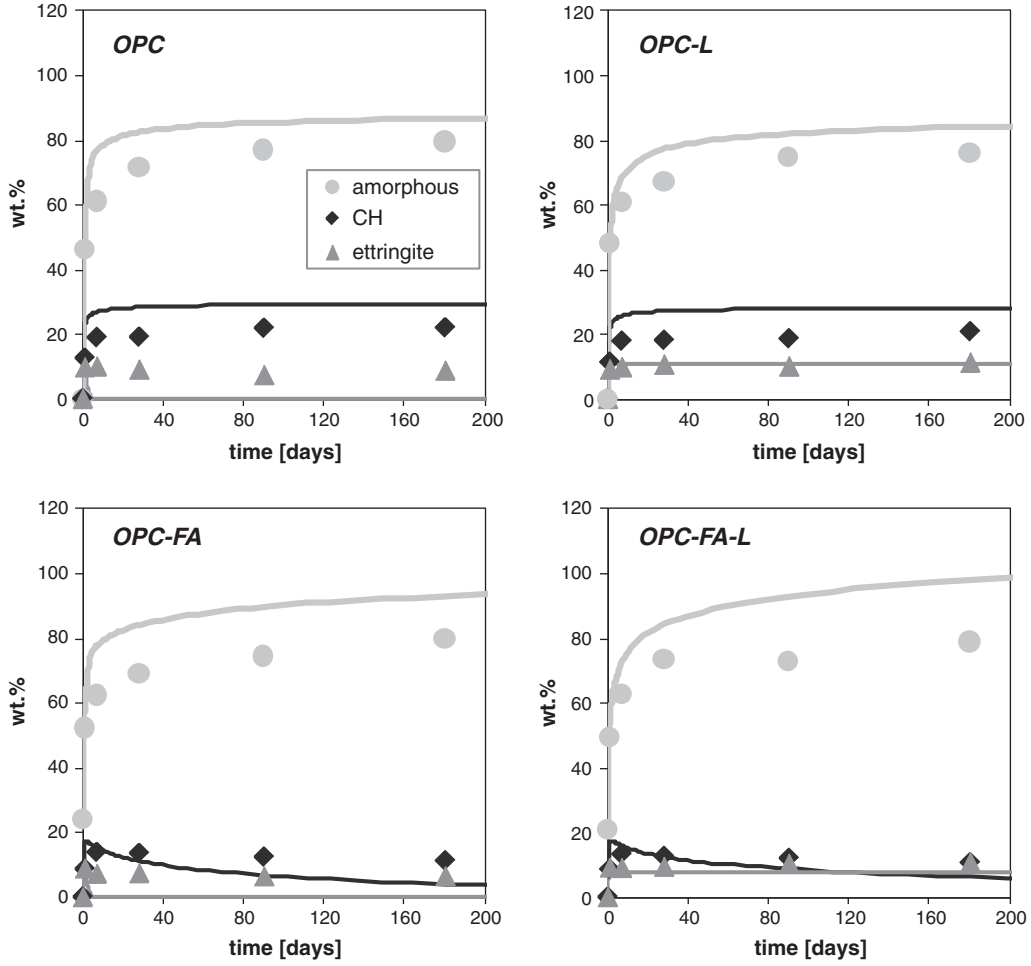

Fig. 14. Comparing XRD-Rietveld (data points) with results calculated by thermodynamic modelling (solid lines) in wt.%, for details see text. Amorphous includes different hydrates (C–S–H, AFm or hydrotalcite-like phases) and the amorphous fly ash.

real C–S–H. The difference is larger for the fly ash containing blends as their C–S–H deviates even more from the one used in the modelled.

Ettringite is predicted to disappear in both the OPC and OPC-FA blend during the first few days of hydration, however ettringite was observed up to 140 days (Fig. 14); instead traces of hydrogarnet were observed by XRD in the pastes older than 28 days. The persistence of ettringite in the experiments is most likely due to slow kinetics of the decomposition of ettringite to monosulphate and differences in local equilibria. The similar solubility of ettringite and monosulphate in cement systems, as visible in the similar effective saturation index (SI) of monosulphate and ettringite (Table 8), confirms the observed slow kinetics.

For the limestone containing blends, OPC-L and OPC-FA-L, the ettringite content is well predicted (Fig. 14). The model predicts only the formation of monocarbonate after 2 to 3 days (Fig. 13) whereas by XRD hemicarbonate was also observed (Fig. 8). This may be attributed to the slow dissolution kinetics of the limestone powder or to the slower formation of monocarbonate than of hemicarbonate.

4.4.2. Chemical shrinkage and porosity

Based on the predicted volume of unhydrated cement and the hydration products (Fig. 13), the chemical shrinkage (CS_t) and the total porosity (P_t) can be calculated (see Figs. 6 and 11).

$$CS_t = \left(V_{OPC+FA+L,t=0} + V_{solution,t=0}\right) - \left(V_{OPC+FA+L,t} + V_{solution,t} + V_{hydrates,t}\right) \quad (6)$$

$$P_t = \frac{\left(V_{OPC+FA+L,t=0} + V_{solution,t=0}\right) - \left(V_{OPC+FA+L,t} + V_{hydrates,t}\right)}{V_{OPC+FA+L,t=0} + V_{solution,t=0}} \quad (7)$$

CS_t is expressed in cm^3 or ml per g OPC, with $V_{OPC+FA+L,t=0}$ is the initial volume of dry material and $V_{solution,\ t=0}$ the initial amount of water added to the system. $V_{OPC+FA+L,t}$ is the remaining volume of anhydrous material at time t, $V_{solution,\ t}$ the remaining solution and $V_{hydrate,\ t}$ the volume of hydrates formed. The total porosity P_t is expressed as a% of the total volume which is assumed to remain constant over time; shrinkage of the sample is not taken into account. The porosity corresponds roughly to the sum of the capillary pores, thereby not including cracks or air voids [33].

The changes in hydration products result in a difference in chemical shrinkage (Fig. 6). The chemical shrinkage (CS) relative to the OPC content tends to increase when limestone is present. This can be attributed to the fact that more free water is bound in ettringite. The modelled chemical shrinkage shows similar trends as the experimental data (Fig. 6), however the observed effect is somewhat smaller than the modelled one. The modelled porosity as a function of hydration time (Fig. 11) indicates that the effect of limestone powder on OPC-FA cement is larger than on OPC cement, which is in line with previous observations. Note that the coarse porosity as measured by SEM-IA represents only a fraction of the capillary porosity.

5. Conclusions

Five percent of limestone powder can have a beneficial effect on the compressive strength of OPC [13]. This study confirms this and

shows that the effect is even more pronounced for the inclusion of 5% limestone powder in fly ash blended cements. The beneficial effect of the limestone powder cannot be solely attributed to a physical effect due to the presence of 5% limestone (additional nucleation sites and higher effective water to cement ratio), as after longer hydration times, no significant differences in the amount of clinker or fly ash reacted were observed between limestone containing and limestone free blends. Additionally, the presence of 5% limestone increases relative to blends containing the same amount of crystalline quartz powder, the amount of bound water and the compressive strength.

The effect of limestone powder on the hydration of OPC and OPC-FA systems tested in this study, therefore, appears to be mainly due to its interaction with the hydration products formed. At 1 day the hydrates formed are similar for all tested combinations: C–S–H, portlandite, ettringite. But after more than 1 day, when the reaction of the clinkers continues while the gypsum has been depleted, the kind and amount of AFm and AFt phases start to differ between the limestone containing and limestone-free OPC and OPC-FA blends. In the absence of limestone powder, ettringite decomposes to monosulphate. However, in the presence of calcium carbonate, the main constituent of limestone powder, the decomposition of ettringite to monosulphate is prevented as monosulphate is rendered unstable and instead calcium mono- or hemicarboaluminate are formed as observed experimentally and predicted by the thermodynamic modelling. The changes in AFm phases are reflected in the sulphur concentrations of pore solution. This effect is well known for OPC, however, this study proofs that the effect is more pronounced for the fly ash blended cement due to a lower SO_3/Al_2O_3 ratio caused by replacing part of the OPC with fly ash which as it reacts introduces additional alumina to the system. As predicted by the thermodynamic modelling, the XRD patterns show a larger amount of AFm and AFt phases when fly ash is present. However, aluminates liberated by fly ash do not go only into AFm and AFt phases as part of it is also incorporated in the C–S–H gel as observed by the increase of the Al/Si ratio of the C–S–H.

The stabilisation of ettringite, when limestone is present, leads to an increase in the volume of hydration products, as can be deduced from the chemical shrinkage results, to a decrease in porosity and thus to an increase in compressive strength. While a clear increase in strength was observed, the experimental determination of the porosity of the cement paste did not show a clear difference between the blends with and without limestone powder, due the relatively large error associated with the measurements.

Acknowledgement

The authors would like to acknowledge COIN, the COncrete INnovation centre (http://www.coinweb.no) for the financial support.

References

[1] L.L. Mayfield, Limestone additions to Portland cement — an old controversy revisited, Cement, Concrete and Aggregates 10 (1988) 3–8.
[2] K.D. Ingram, K.E. Daugherty, A review of limestone additions to Portland cement and concrete, Cement and Concrete Composites 13 (1991) 165–170.
[3] P. Hawkins, P. Tennis, R. Detwiler, The use of limestone in Portland cement: a state-of-the-art review, EB227, Portland Cement Association, Skokie, Illinois, USA, 2003, p. 44.
[4] T. Schmidt, B. Lothenbach, M. Romer, J. Neuenschwander, K. Scrivener, Physical and microstructural aspects of sulfate attack on ordinary and limestone blended Portland cements, Cement and Concrete Research 39 (2009) 1111–1121.
[5] V.S. Ramachandran, Thermal analyses of cement components hydrated in the presence of calcium carbonate, Thermochimica Acta 127 (1988) 385–394.
[6] G. Kakali, S. Tsivilis, E. Aggeli, M. Bati, Hydration products of C_3A, C_3S and Portland cement in the presence of $CaCO_3$, Cement and Concrete Research 30 (2000) 1073–1077.
[7] J. Bensted, Further hydration investigations involving Portland cement and the substitution of limestone for gypsum, World Cement 14 (1983) 383–392.
[8] W. Klemm, L. Adams, An investigation on the formation of carboaluminate, in: P. Klieger, D. Hooton (Eds.), ASTM Spec Tech Publ, 1064, 1990.
[9] T. Matschei, F.P. Glasser, Temperature dependence, 0 to 40 °C, of the mineralogy of Portland cement paste in the presence of calcium carbonate, Cement and Concrete Research 40 (2010) 763–777.
[10] H.J. Kuzel, H. Pöllmann, Hydration of C_3A in the presence of $Ca(OH)_2$, $CaSO_4 \cdot 2H_2O$ and $CaCO_3$, Cement and Concrete Research 21 (1991) 885–895.
[11] S. Hoshino, K. Yamada, H. Hirao, XRD/Rietveld analysis of the hydration and strength development of slag and limestone blended cement, Journal of Advanced Concrete Technology 4 (2006) 357–367.
[12] T. Matschei, B. Lothenbach, F.P. Glasser, The role of calcium carbonate in cement hydration, Cement and Concrete Research 37 (2007) 551–558.
[13] B. Lothenbach, G. Le Saout, E. Gallucci, K. Scrivener, Influence of limestone on the hydration of Portland cements, Cement and Concrete Research 38 (2008) 848–860.
[14] B. Yilmaz, A. Olgun, Studies on cement and mortar containing low-calcium fly ash, limestone, and dolomitic limestone, Cement and Concrete Composites 30 (2008) 194–201.
[15] M. Ghrici, S. Kenai, M. Said-Mansour, Mechanical properties and durability of mortar and concrete containing natural pozzolana and limestone blended cements, Cement and Concrete Composites 29 (2007) 542–549.
[16] G. Menéndez, V. Bonavetti, E.F. Irassar, Strength development of ternary blended cement with limestone filler and blast-furnace slag, Cement and Concrete Composites 25 (2003) 61–67.
[17] M.F. Carrasco, G. Menéndez, V. Bonavetti, E.F. Irassar, Strength optimization of "tailor-made cement" with limestone filler and blast furnace slag, Cement and Concrete Research 35 (2005) 1324–1331.
[18] K. De Weerdt, H. Justnes, Microstructure of binder from the pozzolanic reaction between lime and siliceous fly ash and the effect of limestone addition, in: W. Sun, K. van Breugel, C. Miao, G. Ye, H. Chen (Eds.), Microstructure Related Durability of Cementitious Composites Nanjing, 2008, pp. 107–116.
[19] K. De Weerdt, H. Justnes, Synergic reactions in triple blended cements, 11th NCB International Seminar on Cement and Building Materials, New Delhi, 2009, pp. 257–261.
[20] K. De Weerdt, H. Justnes, Synergy in ternary cements — the interaction between limestone powder and fly ash, in: L. Black, P. Purnell (Eds.), 29th Cement and Concrete Science Conference, Leeds, UK, 2009, pp. 153–156.
[21] K. De Weerdt, E.J. Sellevold, H. Justnes, K.O. Kjellsen, Fly ash-limestone ternary cements: effect of component fineness., Advances in cement research (accepted), (2010).
[22] K. De Weerdt, H. Justnes, K.O. Kjellsen, E. Sellevold, Fly ash - limestone ternary composite cements: synergetic effect at 28 days, Nordic Concrete Research 42 (2010).
[23] K. De Weerdt, K.O. Kjellsen, E.J. Sellevold, H. Justnes, Synergistic effect between fly ash and limestone powder in ternary cements, Cement and Concrete Composites 33 (2011) 30–38.
[24] M. Geiker, Studies of Portland cement hydration: measurements of chemical shrinkage and a systematic evaluation of hydration curves by means of the dispersion model. Ph.D Thesis, in, Technical University of Denmark, Copenhagen, 1983.
[25] G. Le Saout, T. Füllmann, V. Kocaba, K. Scrivener, Quantitative study of cementitous materials by X-ray diffraction/Rietveld analysis using an external standard, 12th International Congress on the Chemistry of Cement Montréal, Canada, 2007, 2007.
[26] M. Ben Haha, K. De Weerdt, B. Lothenbach, Quantification of the degree of reaction of fly ash, Cement and Concrete Research 40 (2010) 1620–1629.
[27] R.S. Barneyback Jr., S. Diamond, Expression and analysis of pore fluids from hardened cement pastes and mortars, Cement and Concrete Research 11 (1981) 279–285.
[28] D. Kulik, GEMS 2 software, http://gems.web.psi.ch/ PSI, Villingen, Switzerland, 2010.
[29] T. Thoenen, D. Kulik, Nagra/PSI chemical thermodynamic database 01/01 for GEMS-selektor (V.2-PSI) geochemical modeling code, http://gems.web.psi.ch/doc/pdf/TM-44-03-04-web.pdf PSI, Villingen, 2003.
[30] W. Hummel, U. Berner, E. Curti, F.J. Pearson, T. Thoenen, Nagra/PSI chemical thermodynamic data base 01/01, Universal Publishers/uPUBLISH.com, USA also published as Nagra Tehcnical Report NTB 02-16, Wettingen, Switzerland 2002, 2002.
[31] B. Lothenbach, F. Winnefeld, Thermodynamic modelling of the hydration of Portland cement, Cement and Concrete Research 36 (2006) 209–226.
[32] T. Matschei, B. Lothenbach, F.P. Glasser, Thermodynamic properties of Portland cement hydrates in the system $CaO–Al_2O_3–SiO_2–CaSO_4–CaCO_3–H_2O$, Cement and Concrete Research 37 (2007) 1379–1410.
[33] B. Lothenbach, T. Matschei, G. Möschner, F.P. Glasser, Thermodynamic modelling of the effect of temperature on the hydration and porosity of Portland cement, Cement and Concrete Research 38 (2008) 1–18.
[34] D.P. Bentz, Modeling the influence of limestone filler on cement hydration using CEMHYD3D, Cement and Concrete Composites 28 (2006) 124–129.
[35] T. Sato, J.J. Beaudoin, The effect of nano-sized $CaCO_3$ addition on the hydration of cement paste containing high volumes of fly ash, 12th ICCC, Montreal, 2007, pp. 1–12.
[36] H.F.W. Taylor, K. Mohan, G.K. Moir, Analytical study of pure and extended Portland cement pastes: II, fly ash- and slag-cement pastes, Journal of the American Ceramic Society 68 (1985) 685–690.
[37] W. Lukas, The influence of an Austrian fly ash on the reaction processes in the clinker phases of Portland cements, Materials and Structures 9 (1976) 331–337.
[38] K. Ogawa, H. Uchikawa, K. Takemoto, I. Yasui, The mechanism of the hydration in the system C_3S-pozzolana, Cement and Concrete Research 10 (1980) 683–696.

[39] E. Sakai, S. Miyahara, S. Ohsawa, S.-H. Lee, M. Daimon, Hydration of fly ash cement, Cement and Concrete Research 35 (2005) 1135–1140.
[40] J.A. Dalziel, W.A. Gutteridge, The influence of pulverized-fuel ash upon the hydration characteristics and certain physical properties of a Portland cement paste, Cement and Concrete Association: Technical Report, Wexham Springs, 1986, p. 28.
[41] T. Matschei, B. Lothenbach, F.P. Glasser, The AFm phase in Portland cement, Cement and Concrete Research 37 (2007) 118–130.
[42] P.L. Rayment, The effect of pulverised-fuel ash on the C/S molar ratio and alkali content of calcium silicate hydrates in cement, Cement and Concrete Research 12 (1982) 133–140.
[43] K. Luke, E. Lachowski, Internal composition of 20-year-old fly ash and slag-blended ordinary Portland cement pastes, Journal of the American Ceramic Society 91 (2008) 4084–4092.
[44] J.I. Escalante-Garcia, J.H. Sharp, The chemical composition and microstructure of hydration products in blended cements, Cement and Concrete Composites 26 (2004) 967–976.
[45] A.M. Harrisson, N.B. Winter, H.F.W. Taylor, An examination some pure and composite Portland cement pastes using scanning electron microscopy with X-ray analytical capability, 8th ICCC, Rio de Janeiro, Brasil, 1986, pp. 170–175.
[46] I. Canham, C.L. Page, P.J. Nixon, Aspects of the pore solution chemistry of blended cements related to the control of alkali silica reaction, Cement and Concrete Research 17 (1987) 839–844.
[47] F.P. Glasser, K. Luke, M.J. Angus, Modification of cement pore fluid compositions by pozzolanic additives, Cement and Concrete Research 18 (1988) 165–178.
[48] S. Diamond, Effects of two Danish flyashes on alkali contents of pore solutions of cement-flyash pastes, Cement and Concrete Research 11 (1981) 383–394.
[49] M.H. Shehata, M.D.A. Thomas, R.F. Bleszynski, The effects of fly ash composition on the chemistry of pore solution in hydrated cement pastes, Cement and Concrete Research 29 (1999) 1915–1920.
[50] D. Herfort, Relationship between strength, porosity and cement composition, Nanocem workshop on “the relation between microstructure and mechanical properties”, Czech Technical University, Prague, 2004.
[51] S. Igarashi, M. Kawamura, A. Watanabe, Analysis of cement pastes and mortars by a combination of backscatter-based SEM image analysis and calculations based on the Powers model, Cement and Concrete Composites 26 (2004) 977–985.
[52] L.J. Parrot, D.C. Killoh, Prediction of cement hydration, British Ceramic Proceedings 35 (1984) 41–53.